ISSN 1067-8212, Russian Journal of Non-Ferrous Metals, 2015, Vol. 56, No. 1, pp. 114–118. © Allerton Press, Inc., 2015.

NANOSTRUCTURED MATERIALS AND FUNCTIONAL COATINGS

Preparation of Nanosized Zinc Oxide by Vacuum Oxidation and Behaviors of Impurity Elements[1]

Rong Liang Zhang*, Ai Bo Shi, and Yun Xue Jin

School of Material Science and Engineering, Jiangsu University of Science and Technology, no. 2, Mengxi Rd., Zhenjiang city, Jiangsu Province, 212003 China

**e-mail: zhangrljx19201@163.com*

Abstract—Nanosized zinc oxide with the purity ≥99.98 was prepared with a vacuum oxidation method based on hot-dip galvanizing slag by using air as the oxygen source. The effects of reaction temperature and vacuum degree on the product morphologies were investigated, and the influences of main impurity elements in raw materials on the quality of products were evaluated under different oxidation conditions. Reaction temperature arid vacuum degree dramatically affect the product morphologies. At appropriate temperature and vacuum degree, the main products are wurtzite crystals. The crystal needles are elongated and long in length. Impurity Fe and Pb elements influence the quality of products through various patterns under different oxidation conditions. Fe remains in the products mainly relying on the mechanical entrainment of Zn vapor and the positive deviation of Fe–Zn system, while Pb is retained mainly based on the vapor pressure and the positive deviation of Pb–Zn system.

Keywords: hot-dip galvanizing slag, nanosized zinc oxide, vacuum degree, impurity element

DOI: 10.3103/S1067821215010204

1. INTRODUCTION

Nanosized zinc oxide is, due to fine crystal grains, novel multifunctional inorganic materials with unique surface electronic structure and crystal structure, thus being characteristic in surface effect, volume effect, quantum size effect, macroscopic quantum tunneling effect, as well as high transparency and dispersion, etc. Being superior to ordinary ZnO, it has been widely applied in the fields of ceramics, chemical engineering, electronics, optics, biology, and medicine, etc. [1]. Currently, nanosized ZnO, which is prepared by expensive high-purity zinc salts or metal zinc [2–4], has not been extensively utilized.

Hot-dip galvanizing slag, which contains over 80% and even over 90% Zn, and impurities such as Fe (3–5%), Al, Sn, Pb, Cd, Cu and Ni [5], is an eligible renewable zinc resource. The slag is commonly subjected to pyrometallurgical process and hydrometallurgical process at present, pyrometallurgical process gives zinc powders, metal zinc and zinc-based alloys mainly by distillation and liquation [6, 7], while hydrometallurgical process produces metal zinc, high-purity ZnO and zinc salts such as zinc sulfate, basic zinc carbonate and zinc phosphate [8–13]. Pyrometallurgical process suffers from low recovery, high energy consumption and severe pollution owing to the high Fe content. Similarly, the application of hydrometallurgical process is limited owing to the high equipment investment and energy consumption, unstable operation, time-consuming steps, complicated protocols, high cost and tendency to secondary pollution. Therefore, using hot-dip galvanizing slag as the raw material is of great significance to direct deep processing of zinc materials and preparation of composite materials by enriching the resources and reducing the production cost simultaneously.

Thereby motivated, we herein fabricated nanosized ZnO, based on the slag and air, by oxidizing zinc vapor at low partial pressure of oxygen in vacuum through regulating the vacuum degree in a reaction chamber.

2. MATERIALS AND METHODS

2.1. Materials and Apparatus

Hot-dip galvanizing slag was provided by Jiangsu XX Factory of China, with its chemical constitution listed in Table 1.

The main apparatus included TCE-II intelligent temperature controller, 2XZ-I rotary vane vacuum pump, DP-AF (vacuum) precision digital pressure gauge, condensing chamber and electrically heated vacuum reaction chamber (prepared in our group, controlled by a thermocouple).

[1] The article is published in the original.

Table 1. Chemical constitution of hot-dip galvanizing slag (mass fraction), %

Constitution	Zn	Ni	Fe	Cd	Mn	Cu	Pb	Al	Sn
Content	95.20	0.024	4.70	0.0003	0.0072	0.0038	<0.005	0.038	<0.001

Table 2. Contents of impurities in products (mass fraction), %

Constitution	Ni	Fe	Cd	Mn	Cu	Pb	Al	Sn
Content	<0.003	0.0031	0.0004	<0.001	<0.001	<0.003	<0.001	<0.001

2.2. Experimental Methods

Hot-dip galvanizing slag plate was cut into small blocks and put in a porcelain boat. The vacuum reaction chamber was heated to 800–950°C when the porcelain boat was pushed in. Then the vacuum degree inside the chamber was regulated by a fine-tuning valve to control the oxygen content. Heating was stopped after 8–10 min of thermal insulation, and the products were collected for analysis after cooling.

Crystal structure was analyzed by Shimadzu XRD-6000 X-ray diffractometer. Morphology was observed and particle size was measured by JSM-7001F thermal field emission scanning electron microscope. Impurity contents were determined by inductively coupled plasma atomic emission spectroscope (IRIS Advantage) and atomic absorption spectrometer (SpectrAA 220FS).

3. RESULTS AND DISCUSSION

3.1. XRD Analysis of Products

The products are soft, white flocs. The XRD results under different reaction conditions are shown in Fig. 1. As evidenced by the sole sharp diffraction peak of ZnO, the products are highly pure as integral, wurtzite crystals without impurity phases. Besides, as shown in Table 2, the purity of products is not lower than 99.98%.

3.2. Effects of Reaction Temperature on Morphology

The morphologies at various temperatures are exhibited in Fig. 2. It can be seen that temperature evidently affected the morphology of products.

Besides needle-like and tetraneedle-like ZnO, there are also a small number of lamellar crystals (Fig. 2a) mainly because of the poor directional crystal growth resulting from the slow growth of crystal nuclei due to the sluggish oxidation at low temperature. Most products are tetraneedle-like crystals at 870°C (Fig. 2b). The diameter at the root is approximately 50 nm, and the lengths range from 0.3 to 4.0 μm, while being elongated and long in length. There are almost no granular or lamellar crystals, and the morphology and sizes are relatively uniform. When the temperature is further risen to 900°C, the crystals grow so rapidly that considerable lamellar ones are generated owing to the quick oxidation that provides sufficient materials for formation of crystal nuclei and crystal growth (Fig. 2c).

3.3. Effects of Vacuum Degree on Morphology

In addition to temperature, vacuum degree also critically influences crystal growth by changing the Zn evaporation rate and the O content, thus determining the gas-phase saturation in the system.

The morphologies at various vacuum degrees are exhibited in Fig. 3. At high vacuum degree (low system pressure), the resultant insufficient oxygen yields a disuniform morphology (Fig. 3a), the needles of which are restricted from vigorous growth. The grayish white products are unoxidized metal zinc. When the oxygen content, which is controlled by the fine-tuning valve, is compatible with the crystal grow rate, the products are uniform, long ZnO nano-tetraneedles (Fig. 3b). However, lamellar crystals are generated instead with decreasing vacuum degree (high system pressure) because the resultant slow evaporation of metal zinc allows the secondary growth of uniform needle-like crystals (Fig. 3c).

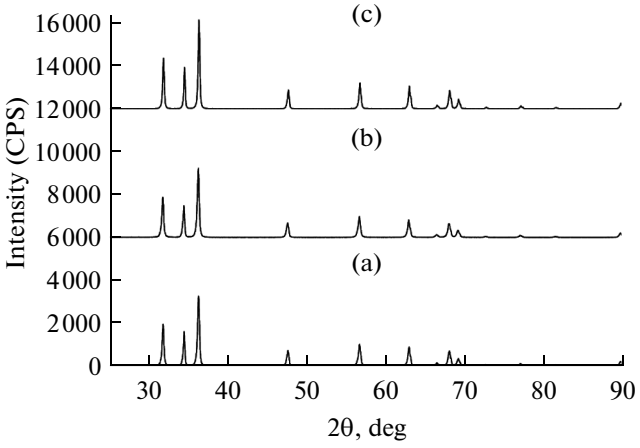

Fig. 1. XRD results of ZnO under different reaction conditions.

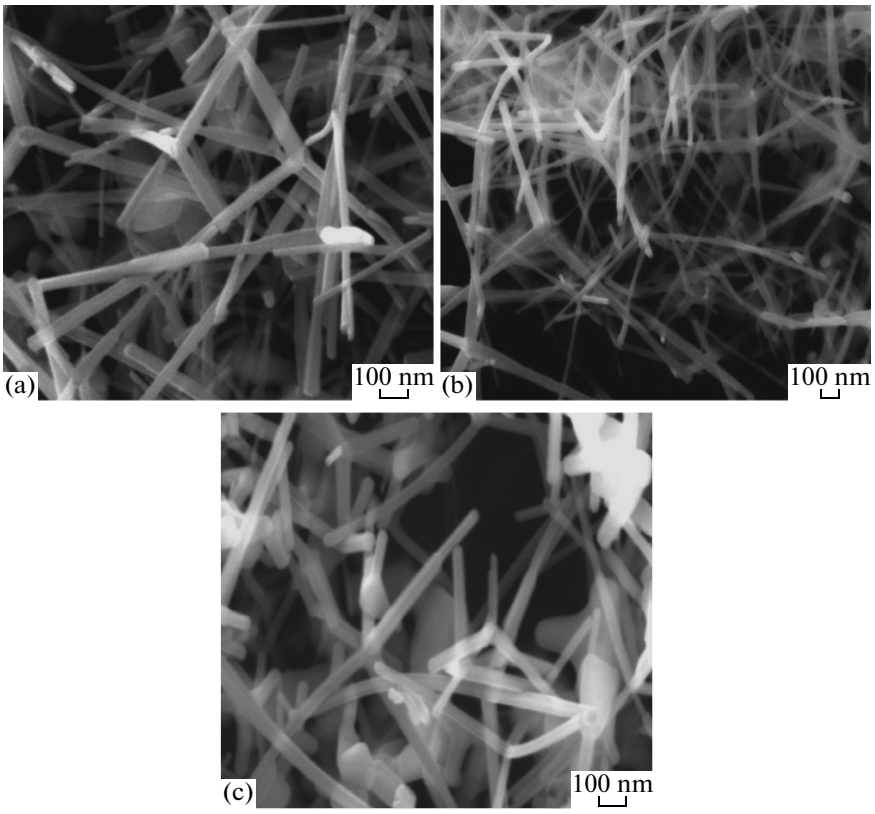

Fig. 2. Effects of reaction temperature on morphology: (a) 800°C; (b) 870°C; (c) 900°C.

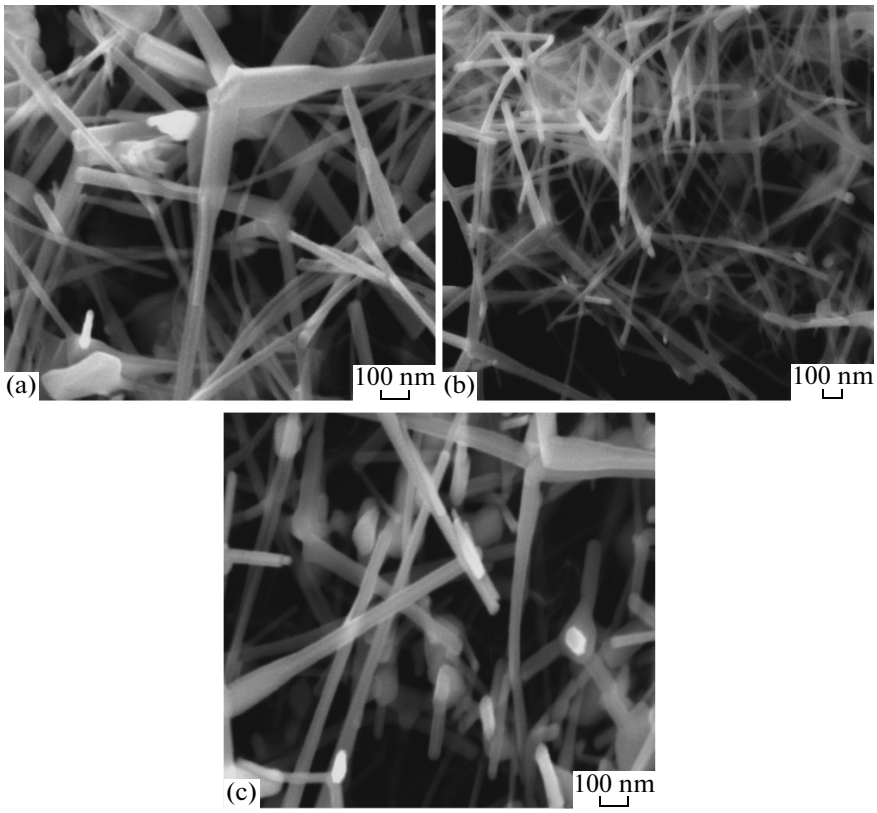

Fig. 3. Effects of vacuum degree on morphology: (a) 19975 Pa; (b) 21975 Pa; (c) 23975 Pa.

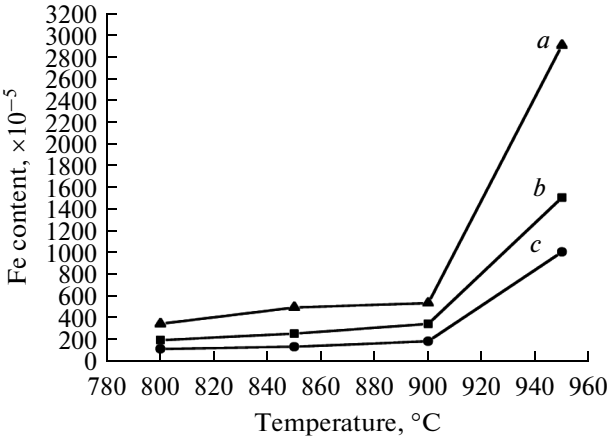

Fig. 4. Relationship between Fe content in products and temperature: (a) 23975 Pa; (b) 21975 Pa; (c) 19975 Pa.

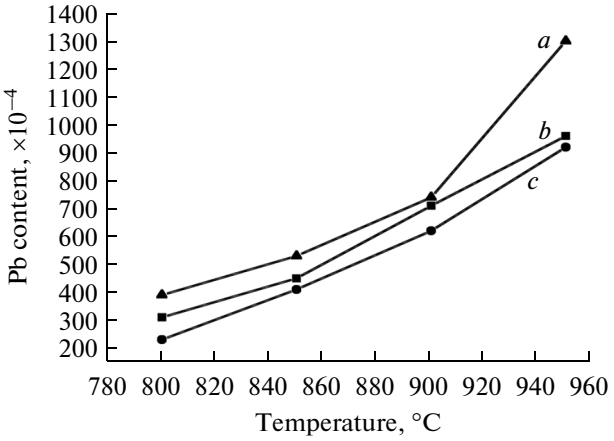

Fig. 5. Relationship between Pb content in products and temperature: (a) 23975 Pa; (b) 21975 Pa; (c) 19975 Pa.

3.4. Behaviors of Impurity Elements

In this study, only the effects of Fe and Pb on the quality of products were evaluated under different oxidation conditions, given that Fe is the main impurity element, and the vapor pressures of Al, Ni, Mn and Cu are over millionfold different from that of Zn. The experimental results are shown in Figs. 4 and 5.

At the same temperature, significantly more Fe is retained in the products with reducing vacuum degree (rising system pressure) (Fig. 4). In contrast, the Fe content only skyrockets at above 900°C at the same vacuum degree.

In the Fe–Zn system, when vacuum-distills at 900°C, merely 10^{-8} of the gaseous substance is Fe with as high as 90% Fe in the liquid phase, suggesting that the vapor pressure of Fe element is negligible herein. Therefore, it is reasonable to infer that mechanical entrainment primarily affects the Fe content in products.

Impurity Fe element is prone to entering the vapor phase with elevating temperature that accelerates the Zn evaporation, and because of, axiomatically, the high Fe content in raw materials. As evidenced by the activity coefficient table [14], the Fe–Zn system shows positive deviation. Subsequently, iron-rich phase is dominant with increasing Fe content in the slag, thus leaving evidently more Fe in products by enhancing mechanical entrainment.

Overall, Fe remains in the products mainly relying on the mechanical entrainment of Zn vapor and the positive deviation effect. Therefore, the evaporation rate of Zn vapor is determinative, which can be controlled by regulating the system vacuum degree, as well as the Zn evaporation amount and temperature.

Besides, the Pb content increases several folds from 800 to 950°C at various vacuum degrees (Fig. 5), revealing that the production of impurity Pb element can mainly be ascribed to the temperature-dependent vapor pressure other than mechanical entrainment. The Pb content in products increases with decreasing vacuum degree (rising system pressure) at a specific temperature, since more Pb may be oxidized into PbO in the presence of higher O content, and in the meantime, the vapor pressure of PbO significantly exceeds that of metal Pb under identical conditions.

Moreover, the Pb–Zn system also shows positive deviation based on the activity diagram [15]. The effect that is initially obvious gradually attenuated thereafter, thus reducing the difference between the vapor pressures of Zn and Pb. Given the Pb vapor pressure is raised more quickly with rising temperature, the Pb content in products increases.

In short, Pb is retained mainly based on the vapor pressure and the positive deviation effect, which thus requires elaborate control of the reaction temperature.

4. CONCLUSIONS

Nanosized ZnO with the purity ≥99.98 was prepared with a vacuum oxidation method based on hot-dip galvanizing slag by using air as the oxygen source. Reaction temperature and vacuum degree remarkably affects the product morphologies. At appropriate temperature and vacuum degree, the main products are uniform, wurtzite crystals. The diameter at the root is approximately 50 nm, and the lengths range from 0.3 to 4.0 μm, while being elongated and long in length. Impurity Fe and Pb elements affect the final quality of products through various patterns under different oxidation conditions. Fe remains in the products mainly relying on the mechanical entrainment of Zn vapor and the positive deviation of Fe–Zn system, while Pb is retained mainly based on the vapor pressure and the positive deviation of Pb–Zn system. Hence, the impurity contents can be minimized by optimizing the reaction temperature and vacuum degree.

REFERENCES

1. Mahuya, C., Jana, D., and Sanyal, D., Positron annihilation characterization of nanocrystalline ZnO, *Vacuum*, 2013, vol. 87, pp. 16–20.
2. Park, H., Tong, E., Sujan, A., Chung, Park, Y.M., Tatarchuk, B.J., Koo, H., Ahn, H., Yoon, Y.S., and Kim, D., Growth of nanostructured ZnO on wearable fabrics for functional garment, *Mater. Lett.*, 2014, vol. 118, pp. 47–50.
3. Abbasi, M.A., Khan, Y., Hussain, S., Nur, O., and Willander, M., Anions effect on the low temperature growth of ZnO nanostructures, *Vacuum*, 2012, vol. 86, pp. 1998–2001.
4. Sangari, N.U. and Devi, S.C., Synthesis and characterization of nano ZnO rods via microwave assisted chemical precipitation method, *J. Solid State Chem.*, 2013, vol. 197, pp. 483–488.
5. Xu, B.Q., Yang, B., Liu, D.C., Dai, Y.N., and Mao, W.H., The study on recovering metal zinc from the hot galvanizing slag by vacuum distillation, *Non-Ferrous Mining Metallurgy (Chin.)*, 2007, vol. 23, pp. 53–55.
6. Ren, Y.S., Li, Y.Q., and Feng, C.B., Study on two-step zinc regeneration technology from zinc slag during hot-dip galvanizing process, *Bao Steel Technol. (Chin.)*, 2003, vol. 1, pp. 60–62.
7. Gu, Z.H. and Zheng, H.J., Investigation progress on hydrometallurgical recovery of zinc from industrial wastes. Hydrometallurgy of China, *Hydrometallurg. China (Chin.)*, 2007, vol. 26, pp. 67–70.
8. Ding, D.L., Liu, J.X., and Han, Y.X., Zinc powders preparation by alkaline electrowinning from hot galvanizing slag, *Nonferrous Met. (Chin.)*, 2007, vol. 59, pp. 43–45.
9. Wu, Z.Y., Fang, Z., Xu, H.Y., Qiu, L.G., and Li, C., Property of optical absorption and bacteria inhibition of nano ZnO prepared by thermo-plating hard Zn with Fe, *Mater. Rev. (Chin.)*, 2009, vol. 23, pp. 54–57.
10. Yuan, X.H., He, M.Y., Wang, S.M., Zhao, X., and Zhao, X.J., Formation cause and recovering technology of hot galvanizing dross, *Yunnan Metallurgy (Chin.)*, 2007, vol. 36, pp. 32–35, 44.
11. Dvorak, P. and Jandova, J., Hydrometallurgical recovery of zinc from hot dip galvanizing ash, *Hydrometallurgy*, 2005, vol. 77, pp. 29–33.
12. Stocks, C., Wood, J., and Guy, S., Minimisation and recycling of spent acid wastes from galvanizing plants, *Resources Conserv. Recycling (Chin.)*, 2005, vol. 44, pp. 153–156.
13. Zheng, H.J., Gu, Z.H., and Zheng, Y.P., Electrorefining zinc dross in ammoniacal ammonium chloride system, *Hydrometallurgy*, 2008, vol. 90, pp. 8–12.
14. Dai, Y.N., *Non-Ferrous Metal Metallurgy and Vacuum Metallurgy*, Beijing: Metallurgical Industry Press, 2009, p. 92.
15. Dai, Y.N. and Zhao, Z., *Vacuum Metallurgy*, Beijing: Metallurgical Industry Press, 1988, p. 17.